Superresolution of two unbalanced point sources assisted by the entangled partner

Abdelali Sajia and Xiao-Feng Qian *

Center for Quantum Science and Engineering and Department of Physics, Stevens Institute of Technology, Hoboken, New Jersey 07030, USA

(Received 12 January 2022; revised 25 June 2022; accepted 18 August 2022; published 29 September 2022)

Sub-diffraction-limit resolution, or superresolution, has been successfully demonstrated in recent theoretical and experimental studies for two equal-brightness and incoherent point sources. However, practical situations of either nonequal brightness (i.e., unbalancedness) or partial coherence are shown to have fatal effects on such superresolution. As a step towards resolving such issues, we consider the effects of both unbalancedness and a form of partial coherence (i.e., quantum state coherence) together by including an entangled degree of freedom of the two point sources. Unexpectedly, it is found that the two negative effects can counteraffect each other, thus permitting credible superresolution, when the measurement is analyzed in the entangled partner's rotated basis. The least resolvable non-zero two-source separation is also identified analytically. Our result represents useful guidance towards the realization of superresolution for practical point sources. The vector-structure analog of quantum and classical light sources also suggests that our analysis applies to both contexts.

DOI: 10.1103/PhysRevResearch.4.033244

I. INTRODUCTION

The resolution of two point sources is one of the most crucial elements in the science of imaging and sensing. The quality of fine resolution relies on two major factors: resolution capability (how small a separation can be discriminated) and measurement estimation credibility (how much a measurement can be trusted). For over a century, the empirical Abbe-Rayleigh diffraction criterion [1–4], related to the ratio of the light wavelength and aperture diameter, has been regarded as a roadblock that limits resolution capability with practically sensible parameters [5,6]. This is due to the fact that when the two sources are getting closer, the blurred overlapping signals are harder to discriminate through direct intensity measurements. Moreover, the second factor, measurement credibility (or measurement precision), will also decrease as noise effects become relatively more prominent when the separation of the two sources decreases. Studies have shown that while statistical methods were able to improve the resolution capability by determining the source locations, the measurement precision vanishes as the separation of the two sources goes beyond the diffraction limit, approaching zero [7–10]. This phenomenon consolidates the common wisdom of the Abbe-Rayleigh diffraction criterion from a more rigorous foundation and is termed Rayleigh's curse by many authors (see, for example, [11–20]).

Recently, the pioneering works of Tsang and coworkers [12,14,21,22] showed that it is possible, in principle, to improve both factors by analyzing the signal in a different spatial basis (e.g., the Hermite-Gaussian mode) instead of a direct intensity measurement. The new technique leaves the Abbe-Rayleigh diffraction criterion irrelevant and at the same time guarantees a finite desired estimation accuracy via the Fisher information (FI) [23,24]. Experimental confirmation has also been demonstrated (see, for example, [15,20]). While working perfectly in ideal situations, this technique has two constraints, requiring (1) incoherence and (2) balance (equal brightness) of the two point sources. It was shown that releasing either one of the two may lead to the resurgence of Rayleigh's curse, by Řehaček *et al.* with unbalanced incoherent sources [16] and by Larson and Saleh [17,25] and De *et al.*, [26] with balanced but partially coherent sources.

To address this issue, we consider both restrictions at the same time by investigating the resolution of two unbalanced and partially coherent (in terms of quantum state coherence) point sources with the assistance of an entangled partner (see the schematic illustration in Fig. 1). The effect of partial coherence is analyzed by basis rotation of the entangled partner, resulting in continuous variation of quantum state coherence [27]. It is found that the effect of unbalancedness on the two-source separation estimation parameter, i.e., Fisher information, is equivalent to that of the basis-rotation-induced partial quantum coherence. Unexpectedly, the joint effect of the two restrictions by entanglement permits the realization of superresolution with finite Fisher information even when the separation of the two sources approaches zero. It is also determined analytically that a "least resolvable" (nonzero) distance at which the Fisher information experiences a nonzero minimum exists that is determined by Lambert $\mathcal{W}$ functions [28]. This provides guidance to employ optimum practical parameters to achieve superresolution with a given accuracy requirement.

*xqian6@stevens.edu

Published by the American Physical Society under the terms of the Creative Commons Attribution 4.0 International license. Further distribution of this work must maintain attribution to the author(s) and the published article's title, journal citation, and DOI.

II. MODEL AND METHODS

We consider two unbalanced sources located at $x \pm s/2$ with a separation s. Through a shift-invariant imaging system,

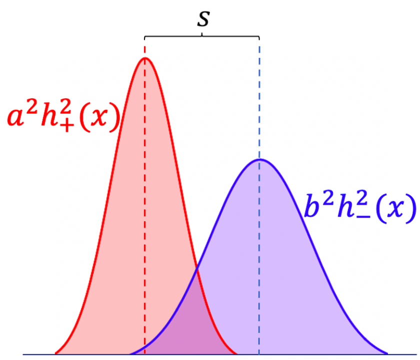

FIG. 1. The point spread functions, $h_+^2(x)$ and $h_-^2(x)$, of two unbalanced point sources separated by s via a shift-invariant imaging system. The coefficients a and b characterize a continuous unbalancedness.

the spatial dependence of the two source amplitudes can be expressed as $h_\pm(x) = h(x \pm s/2)$. Here $h^2(x)$ describe the normalized point spread functions, e.g., taking the Gaussian form $h^2(x) = \frac{1}{\sqrt{2\pi\sigma^2}}\exp[-\frac{x^2}{2\sigma^2}]$, with σ being the width (see the illustration in Fig. 1). We include the partial coherence property of the two sources by introducing an entangled partner of the spatial degree of freedom. The optical field in the image plane can then be described as

$$|\Psi_{\rm ent}\rangle = a\,|h_+\rangle\,|\phi_1\rangle + be^{i\varphi}\,|h_-\rangle\,|\phi_2\rangle, \tag{1}$$

where $|h_\pm\rangle$ represent the two normalized but nonorthogonal functions (vectors) of the spatial degree of freedom, with $\langle x\,|h_\pm\rangle = h_\pm(x)$ and $\langle h_+|h_-\rangle = \delta$; $|\phi_1\rangle$ and $|\phi_2\rangle$ are two generic states describing the remaining degrees of freedom (including polarization, temporal domain, etc.); a and b are real normalized coefficients, with $a^2 + b^2 = 1$; and φ is an arbitrary phase. The spatial functions $h_\pm(x)$ can represent the probability amplitude distributions for a quantum wave function or the field amplitudes of a classical light. Since the spatial functions are normalized over the entire space, the degree of unbalancedness of the two sources can be simply quantified by the ratio $r = |b/a|$, where $r = 0$ means completely unbalanced and $r = 1$ indicates balanced. Due to symmetry, we analyze the case in which that ratio is $r \leqslant 1$ without loss of generality. Here the spatial state space $\{|h_+\rangle, |h_-\rangle\}$ is entangled with the remaining state space $\{|\phi_1\rangle, |\phi_2\rangle\}$. The entangled state (1) can be either a quantum state of single photons or a macroscopic classical optical field [29–38].

For the convenience of the following discussion, we take the two states $|\phi_1\rangle$ and $|\phi_2\rangle$ to be orthogonal and analyze the two-source separation measurements (detections) through the two possible outcomes, i.e., $|\phi_1\rangle$ and $|\phi_2\rangle$, of the nonspatial degree of freedom. Then the degree of coherence with respect to the spatial vectors is taken to be the off-diagonal element of the reduced density matrix (see Ref. [27]),

$$\rho_{\rm spatial} = \begin{pmatrix} a^2 + b^2|\delta|^2 & b^2\delta\sqrt{1-|\delta|^2} \\ b^2\delta^*\sqrt{1-|\delta|^2} & b^2(1-|\delta|^2) \end{pmatrix}, \tag{2}$$

in the basis $\{|h_+\rangle, |h_+^\perp\rangle\}$, with $|h_-\rangle = \delta|h_+\rangle + \sqrt{1-|\delta|^2}|h_+^\perp\rangle$ and $\langle h_+|h_+^\perp\rangle = 0$.

For generality, we further consider the generalized situation in which the measurements are analyzed in the rotated basis of $|\phi_1\rangle$ and $|\phi_2\rangle$, i.e., $|\phi_1^\alpha\rangle = \cos\alpha|\phi_1\rangle - \sin\alpha|\phi_2\rangle$ and $|\phi_2^\alpha\rangle = \sin\alpha|\phi_1\rangle + \cos\alpha|\phi_2\rangle$. The optical field can then be rewritten in the new basis as

$$|\Psi_{\rm ent}\rangle = |h_1\rangle\,|\phi_1^\alpha\rangle + |h_2\rangle\,|\phi_2^\alpha\rangle, \tag{3}$$

where $|h_1\rangle = a\cos\alpha\,|h_+\rangle - b\sin\alpha e^{i\varphi}\,|h_-\rangle$ and $|h_2\rangle = a\sin\alpha\,|h_+\rangle + b\cos\alpha e^{i\varphi}\,|h_-\rangle$ are two new spatial functions that are, in general, non-normalized and nonorthogonal $\langle h_1|h_2\rangle = \delta'$. This is an equivalent way of introducing coherence change due to its basis-dependent nature [27,33,34,38], as the off-diagonal elements of the reduced density matrix for the new spatial states $|h_1\rangle$ and $|h_2\rangle$ will be dependent on the rotation angle α through δ'; a detailed analysis is given in Appendix A 1.

To quantify the likelihood of the estimation being accurate (or the degree to which measurements can be trusted) for the two-source separation s, the conventional FI [23,39,40] is employed. Its definition is based on the Cramér-Rao bound [41–43] $\mathrm{Var}(s) \geqslant 1/F$. The optimal estimation of the unknown parameter s corresponds to the maximization of the Fisher information F, which corresponds to a minimum of the estimator variance $\mathrm{Var}(s)$. Here the estimator is unbiased, which is a condition of the Cramér-Rao bound.

A recent debate about the nonphysical divergence of Fisher information [17,18,22,25] suggests that the Fisher information for analyzing two-source superresolution needs to be appropriately normalized. Here we adopt the approach proposed by Hradil *et al.* [18] to account for the total FI as a sum of weighted components for all probabilistic events. For the general entangled state (3), the FI is defined as

$$F_{\rm tot} = \langle h_1|h_1\rangle F_{\rho_1} + \langle h_2|h_2\rangle F_{\rho_2}, \tag{4}$$

where $\rho_1 = |h_1\rangle\langle h_1|/N_1$ and $\rho_2 = |h_2\rangle\langle h_2|/N_2$ are two corresponding normalized states, by factors N_1 and N_2, of the spatial domain with corresponding weights $\langle h_1|h_1\rangle$ and $\langle h_2|h_2\rangle$. Here the Fisher information takes the form $F_\rho = 2\mathrm{Tr}\{[\partial_s\rho(s)]^2\}$ for an arbitrary pure state $\rho(s) = |h\rangle\langle h|$. This measure is based on the conditional outcome of a measurement in the rotated basis $\{|\phi_1^\alpha\rangle, |\phi_2^\alpha\rangle\}$ of the entangled partner.

It is important to note that here we treat the measurement of the signal as a single repetition (e.g., an independent single-photon detection event, detecting a bunch of identical photons within the coherence time, or a single measurement of light intensity). For a given number (e.g., N) of multiple repetitions of measurement, our results will remain the same up to the constant factor N. Our analysis does not cover environment-induced loss cases where the photon numbers are unknown.

III. RESULTS

In our consideration, the unbalancedness of the two sources $r = |b/a|$ is also an unknown parameter. However, it will be shown later that measurement in the rotated basis $\{|\phi_1^\alpha\rangle, |\phi_2^\alpha\rangle\}$ is always able to cancel the unbalancedness effect. Therefore, one needs to consider only the single unknown parameter s for the calculation of the Fisher information. Then the Fisher information for the entangled field (3) can be explicitly

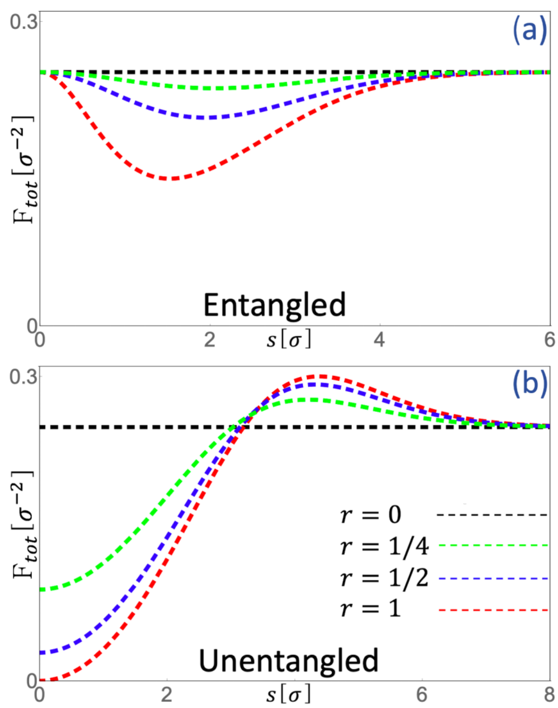

FIG. 2. Dependence of the FI on the displacement s for $\varphi = 0$ with $\sigma = 1$. Different colors represent different values of r. The red line is for the balanced case ($r = 1$), and the blue and green lines corresponds to $r = \frac{1}{2}$, and $r = \frac{1}{4}$, respectively. $r = 0$ is represented by the black line. (a) FI for the state $|\Psi_{\mathrm{ent}}\rangle$ in the case $\alpha = \frac{\pi}{6}$. (b) FI is for the state $|\Psi'\rangle$.

obtained as

$$F_{\mathrm{tot}}(s) = \frac{1}{4\sigma^2} - \frac{(r\sin 2\alpha\cos\varphi)^2 s^2}{16\left[(\cos^2\alpha + r^2\sin^2\alpha)e^{s^2/8\sigma^2} - r\sin 2\alpha\cos\varphi\right]} \times \frac{1}{(r^2\cos^2\alpha + \sin^2\alpha)e^{s^2/8\sigma^2} + r\sin 2\alpha\cos\varphi}, \quad (5)$$

which depends on the two-source separation s, the entangled partner's measurement basis characterized by rotation angle α, the two-source unbalancedness through the amplitude ratio r, and the relative phase φ. Figure 2(a) illustrates the specific behaviors of the Fisher information on s for a fixed partial coherence (rotation angle $\alpha = \pi/6$) and relative phase $\varphi = 0$ but for different unbalancedness $r = 0, 1/4, 1/2, 1$. Qualitative behaviors for other degrees of partial coherence (i.e., other rotation angles) are similar to those in Fig. 2(a) except for some special cases which will be discussed later. The detailed derivation of (5) is provided in Appendix A 2.

Three important conclusions can be drawn from the obtained Fisher information (5) for the entangled source.

The first major conclusion from result (5) is that superresolution is achievable for various practical unbalancedness settings as the value of the Fisher information remains finite even when the separation s goes to zero, as shown in Fig. 2(a). This unexpected behavior is a result of the existence of the entangled partner. To have a clearer picture of the effects of the entangled partner, we also analyze the Fisher information of two unentangled point sources with the same unbalancedness characterized by $r = |b/a|$ and relative phase φ, i.e.,

$$|\Psi'\rangle = (a\,|h_+\rangle + be^{i\varphi}\,|h_-\rangle)|\phi\rangle, \quad (6)$$

where $|\phi\rangle$ is a generic state of the remaining degrees of freedom. In this nonentangled case, the measurement basis of $|\phi\rangle$ is irrelevant to the spatial domain. Therefore, the Fisher information can be directly computed as $F_{\rho'} = 2\mathrm{Tr}[(\partial_s\rho')^2]$, where $\rho' = |\Psi'\rangle\langle\Psi'|/N'$, with N' being the normalization factor. It can be obtained straightforwardly as

$$F_{\rho'}(s) = \frac{\frac{1}{4\sigma^2} - ab\cos\varphi e^{-\frac{s^2}{8\sigma^2}}\frac{(-s^2+4\sigma^2)}{8\sigma^4}}{1 + 2ab\cos\varphi e^{-s^2/8\sigma^2}} - \frac{1}{4}\frac{\left(ab\cos\varphi e^{-\frac{s^2}{8\sigma^2}}s\right)^2}{(1 + 2ab\cos\varphi e^{-s^2/8\sigma^2})^2}. \quad (7)$$

Figure 2(b) illustrates the specific behaviors of $F_{\rho'}$ for the nonentangled field with the same unbalancedness values and fixed phase φ. A detailed derivation of the above result is also provided in Appendix A 3.

By comparing the Fisher information of the two cases illustrated in Figs. 2(a) and 2(b), one notes clearly that the entangled field has a significant enhanced FI for all unbalancedness values in the small separation s regime. Particularly, for the frequently studied balanced source case ($r = 1$), the nonentangled field Fisher information vanishes at zero separation, while the entangled field one achieves its maximum finite value. It is also interesting to note that for the entangled field case, the Fisher information of various different unbalances simply converges to the same finite value when the source separation decreases to zero.

The second major conclusion from result (5) lies in the underlying competing mechanism between coherence and unbalancedness in affecting the Fisher information. As concluded in previous studies, neither partial coherence nor unbalancedness is able to achieve superresolution [16,17]. Surprisingly, as is shown here, the combination of the two works! This is due to the fact that coherence (measured in terms of the quantum state off-diagonal element) and unbalancedness have countereffects against each other on the Fisher information.

To understand this point better, we perform a detailed analysis of the effects from both properties to explore the analogous behavior of the two. We first analyze the coherence effect by fixing at the two-source balanced case, i.e., setting the unbalancedness parameter to $r = 1$. Then the Fisher information simply reduces to

$$F_{\mathrm{tot}}(s, r = 1) = \frac{1}{4\sigma^2} - \frac{1}{16}\frac{\sin^2 2\alpha\cos^2\varphi s^2}{e^{s^2/4\sigma^2} - \sin^2 2\alpha\cos^2\varphi}, \quad (8)$$

which depends on the coherence controlling angle α and two-source separation s. Figure 3(a) illustrates its behavior for different coherence parameter values for α.

Next, we analyze the unbalancedness effect by fixing the coherence rotation angle $\alpha = \pi/4$. To make the comparison we define the unbalancedness parameter as $r = |b/a| = \tan\eta$, where $a = \cos\eta$ and $b = \sin\eta$ to satisfy the normalization condition $a^2 + b^2 = 1$. Then the Fisher information

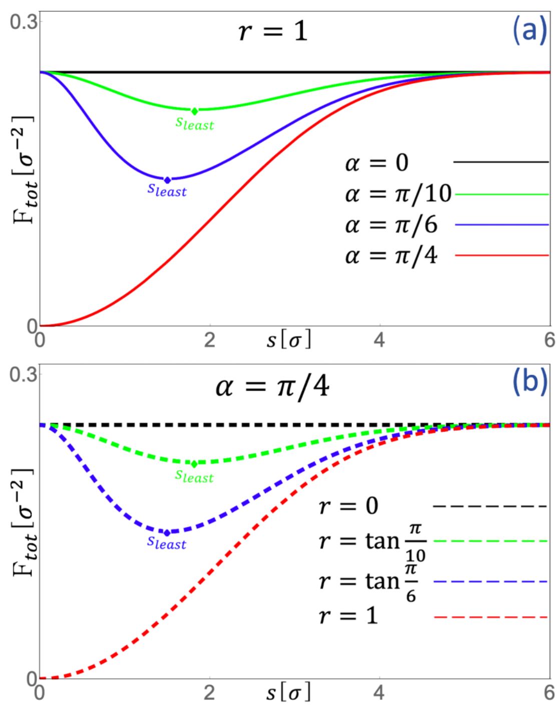

FIG. 3. Total FI versus the displacement s for $\varphi = 0$ when $\sigma = 1$. (a) Rotating basis angle α effect on FI in the balanced case. The minimum of the FI corresponds to s_{least} in expression (11). (b) Unbalancedness intensity effect in the case of $\alpha = \frac{\pi}{4}$.

reduces to

$$F_{\text{tot}}\left(s, \alpha = \frac{\pi}{4}\right) = \frac{1}{4\sigma^2} - \frac{1}{16}\frac{\sin^2 2\eta \cos^2 \varphi s^2}{e^{s^2/4\sigma^2} - \sin^2 2\eta \cos^2 \varphi}, \quad (9)$$

which depends on the unbalancedness angle η and two-source separation s. Figure 3(b) illustrates the behavior for different unbalancedness values of r or, equivalently, η.

By comparing expressions (8) and (9), one immediately notes that they are equivalent except for the change from parameter α to η. This shows that unbalancedness and the rotation-controlled coherence affect the Fisher information with the same mechanism. Therefore, the opposite variations of the two parameters are able to cancel each other's negative effects on the Fisher information, thus permitting a superresolution. Figures 3(a) and 3(b) illustrate specifically the equivalence of the two Fisher information behaviors. When the parameters are chosen appropriately, the two effects behave exactly the same, as shown by lines with the same color in the two plots. In addition, using the fact that angle α is controllable by the analyzer, one can always achieve finite FI for an arbitrary unknown parameter r, as shown in Fig. 3. This justifies that in the calculation of the Fisher information (5), it is not necessary to estimate the unknown parameter r.

Also, we observe that in the limit $s \to 0$, Fisher information $F_{\text{tot}}(s, r)$ will never vanish for any unbalanced (i.e., $r \neq 1$) sources; a detailed proof is given in Appendix A 4. From the equivalence of the coherence and unbalancedness effect, it can therefore be concluded that by adjusting the coherence rotation angle α one can always avoid the balanced situation and thus avoid the vanishing Fisher information at zero separation.

The third major conclusion from the Fisher information (5) is its counterintuitive decreasing behavior within the small separation regime [see illustrations in Figs. 2(a) and 3]. Normally, one would expect that as the separation s of the two sources increases, the Fisher information would also increase because it is natural to assume that a larger separation means less relative error in measurements. However, as shown in Figs. 2(a) and 3, the Fisher information experiences a decrease and then an increase as the separation s increases from zero. This behavior is due to the competing natures of coherence α and unbalancedness r in affecting the Fisher information for any fixed relative phase φ.

This interesting behavior suggests the existence of a least resolvable separation s_{least} that leads to minimum Fisher information $F_{\text{tot}}^{\text{min}}$. All practical situations should avoid analyzing distances in the vicinity of this critical separation s_{least}. To achieve this separation quantitatively, we analyze the derivative of the Fisher information (5). The vanishing derivative of F_{tot} leads to the solutions of the following equation:

$$\Lambda(s)e^{s^2/4\sigma^2} + \Pi(s)e^{s^2/8\sigma^2} + \Omega = 0, \quad (10)$$

where $\Lambda(s) = (a^2\cos^2\alpha + b^2\sin^2\alpha)(b^2\cos^2\alpha + a^2\sin^2\alpha)(1 - \frac{2s^2}{8\sigma^2})$, $\Pi(s) = [2(a^2\cos^2\alpha + b^2\sin^2\alpha) - 1](1 - \frac{s^2}{8\sigma^2})$ $ab\sin 2\alpha\cos\varphi$, and $\Omega = -(ab\sin 2\alpha\cos\varphi)^2$. There are two trivial solutions, $s = 0$ and $s \to \infty$, as shown in Figs. 2(a) and 3. The nontrivial solution can, in general, always be achieved numerically. For the commonly studied balanced case in which $r = 1$, the nontrivial solution of (10) can be obtained analytically as (see the detailed analysis in Appendix A 5)

$$s_{\text{least}} = \sigma\sqrt{4 + 4\mathcal{W}\left[-\frac{\sin^2 2\alpha\cos^2\varphi}{e}\right]}, \quad (11)$$

where $\mathcal{W}[\cdot]$ is a special function known as the Lambert $\mathcal{W}$ function which is an increasing function with a minimum at $\mathcal{W}[\frac{-1}{e}] = -1$. When $\sin^2 2\alpha\cos^2\varphi = 1$, $s_{\text{least}} = 0$, which is exactly the case analyzed in [18] for $\varphi = 0, \pi$ and $\alpha = \pi/4$.

Due to the equivalence of the coherence effect and unbalancedness effect as analyzed earlier, the least resolvable distance with respect to different values of the parameter r can be obtained in exactly the same way as (11); see the illustrations of s_{least} for different curves in Figs. 3(a) and 3(b). Since the detection basis (in terms of α) can be controlled by the observer, all unbalanced cases can be treated equivalently to balanced cases but with a corresponding coherence angle α. The least resolvable distance analysis provides important guidance for avoiding resolution of the two-source separation in the vicinity of s_{least} in various practical situations.

Finally, we would like to mention that our model described in state (1) has direct practical implications. The Gaussian point spread function is a practically feasible fitting of the position of most fluorescent emitters in localization microscopy, which justifies the spatial functions $|h_+\rangle$ and $|h_-\rangle$. The remaining degrees of freedom in many cases can be taken as just the polarization properties of the sources, e.g., $|\phi_1\rangle = |H\rangle$ and $|\phi_2\rangle = |V\rangle$. Then it is straightforward to perform rotations and detections of the signal, thus realizing superresolution.

IV. CONCLUSION AND DISCUSSION

To summarize, we have investigated sub-diffraction-limit resolution of two point sources in two practical situations: arbitrary two-source unbalancedness and partial quantum coherence. By including an entangled partner of the spatial property of the two sources to account for the partial coherence, it was found that superresolution can be achieved with high measurement estimation credibility (quantified by the maximum Fisher information) even when the two-source separation is reduced to zero. It was revealed that such an achievement is due to the fact that the effect on Fisher information from partial coherence is equivalent to that of the two-source unbalancedness. Appropriate control of the rotated basis (i.e., adjustment of quantum state coherence) by the analyzer is able to counter the effect of arbitrary unbalancedness. Such a capability indicates that the realization of superresolution is independent of whether the unbalancedness and partial coherence are known or not. This justifies the exclusion of the unknown unbalancedness and partial coherence parameters in analyzing Fisher information.

We also carried out a detailed analysis of the counterintuitive decreasing behavior of the Fisher information as the two-source separation increases. This allowed the discovery of a characteristic equation to determine the least resolvable distance. Analytical solutions in terms of the Lambert $\mathcal{W}$ function were also achieved. Our results provide important guidance for practical optical designs and engineering in the realization of optimum fine resolution.

ACKNOWLEDGMENTS

We acknowledge partial support from the U.S. Army under Contact No. W15QKN-18-D-0040 and from Stevens Institute of Technology.

APPENDIX

1. Degree of coherence in a rotated basis

Coherence is an important parameter in the analysis of superresolution. Here we adopt the measure for coherence from the quantum state analysis [27]. The optical field in the image plane of the two point sources analyzed in the main text is described as

$$|\Psi_{\rm ent}\rangle = a\,|h_+\rangle\,|\phi_1\rangle + be^{i\varphi}\,|h_-\rangle\,|\phi_2\rangle, \tag{A1}$$

where $|h_+\rangle$ and $|h_-\rangle$ describe the (vector) functions of the spatial degree of freedom and $|\phi_1\rangle$ and $|\phi_2\rangle$ in general are two (vector) functions of the rest of the degrees of freedom and are taken to be orthogonal. As described in the main text, the degree of coherence with respect to the spatial vectors is taken to be the off-diagonal element $|(\rho_{\rm spatial})_{12}| = |b^2\delta\sqrt{1-|\delta|^2}|$ of the reduced density matrix (see Ref. [27]),

$$\rho_{\rm spatial} = \begin{pmatrix} a^2 + b^2|\delta|^2 & b^2\delta\sqrt{1-|\delta|^2} \\ b^2\delta^*\sqrt{1-|\delta|^2} & b^2(1-|\delta|^2) \end{pmatrix}, \tag{A2}$$

expressed in the basis $\{|h_+\rangle, |h_+^\perp\rangle\}$, with $|h_-\rangle = \delta|h_+\rangle + \sqrt{1-|\delta|^2}|h_+^\perp\rangle$ and $\langle h_+|h_+^\perp\rangle = 0$.

The existence of the entangled partner $\{|\phi_1\rangle, |\phi_2\rangle\}$ allows the measurement of the two sources in its rotated basis,

$$|\phi_1^\alpha\rangle = -\sin\alpha\,|\phi_2\rangle + \cos\alpha\,|\phi_1\rangle, \tag{A3}$$

$$|\phi_2^\alpha\rangle = \cos\alpha\,|\phi_2\rangle + \sin\alpha\,|\phi_1\rangle. \tag{A4}$$

This will lead to the optical field being analyzed in a different basis, i.e.,

$$|\Psi_{\rm ent}\rangle = |h_1\rangle\,|\phi_1^\alpha\rangle + |h_2\rangle\,|\phi_2^\alpha\rangle, \tag{A5}$$

where

$$|h_1\rangle = a\cos\alpha\,|h_+\rangle - b\sin\alpha e^{i\varphi}\,|h_-\rangle, \tag{A6}$$

$$|h_2\rangle = a\sin\alpha\,|h_+\rangle + b\cos\alpha e^{i\varphi}\,|h_-\rangle, \tag{A7}$$

and $\langle h_1|h_2\rangle = \delta' = (a^2-b^2)\sin\alpha\cos\alpha + ab\delta e^{i\varphi}\cos^2\alpha - abe^{-i\varphi}\sin^2\alpha\delta^*$.

Due to this rotated detection, the reduced density matrix of the spatial states needs to be analyzed in the new basis, $|h_1\rangle$, $|h_1^\perp\rangle$ (where $|h_2\rangle = \delta'|h_1\rangle + \sqrt{1-|\delta'|^2}|h_1^\perp\rangle$ and $\langle h_1|h_1^\perp\rangle = 0$), and becomes

$$\rho'_{\rm spatial} = \begin{pmatrix} (1+|\delta'|^2)/2 & \delta'\sqrt{1-|\delta'|^2} \\ \delta'^*\sqrt{1-|\delta'|^2} & (1-|\delta'|^2)/2 \end{pmatrix}. \tag{A8}$$

As a result, the off-diagonal element will change accordingly depending on the rotation angle α through δ'. This ensures that analyzing the two sources in a different basis will effectively produce a different partial coherence. In other words, partial coherence, due to its basis-dependent nature [27], can be introduced through rotations of the entangled partner for analysis.

2. Fisher information of the entangled field

Here we derive the expression for Fisher information (FI) in (5) of the main text. When the optical field is analyzed in the rotated basis $|\phi_1^\alpha\rangle, |\phi_1^\alpha\rangle$ of the entangled partner, it can be expressed in the form of (A5). Then FI is calculated based on the conditional measurement on $|\phi_1^\alpha\rangle$ or on $|\phi_2^\alpha\rangle$. Information will be stored in two subsystems considering the weights for each of $|h_1\rangle$ and $|h_2\rangle$, i.e.,

$$F_{\rm tot} = \langle h_1|h_1\rangle F_{\rho_1} + \langle h_2|h_2\rangle F_{\rho_2}, \tag{A9}$$

where F_{ρ_1} and F_{ρ_2} are FI for $\rho_1 = |h_1\rangle\langle h_1|$ and $\rho_2 = |h_2\rangle\langle h_2|$, respectively.

We start with the calculation of a general state in the form $|\Phi\rangle = a'\,|h_+\rangle + b'e^{i\varphi}\,|h_-\rangle$, where $a'^2 + b'^2$ is not necessarily normalized. The point spread functions $|h_\pm\rangle$ can be described as a displacement of a function $|h\rangle$ at the center, i.e., $|h_\pm\rangle = \exp(\pm iPs/2)\,|h\rangle$ and $|\langle x|h\rangle|^2 = \frac{1}{\sqrt{2\pi\sigma^2}}\exp[-\frac{x^2}{2\sigma^2}]$. Here P is the displacement operator, and s is the separation of the two sources.

The Fisher information of such a state $|\Phi\rangle$ can be computed as

$$F_{|\Phi\rangle}(s) = \frac{4}{N}\langle\partial_s\Phi|\partial_s\Phi\rangle - \frac{4}{N^2}|\langle\Phi|\partial_s\Phi\rangle|^2, \tag{A10}$$

where the first term on the right-hand side (RHS) of the equation is given as

$$\langle\partial_s\Phi|\partial_s\Phi\rangle = \langle h|\,iP\tfrac{1}{2}(a'e^{-i\varphi}e^{iP\frac{s}{2}} - b'e^{-iP\frac{s}{2}}) \times iP\tfrac{1}{2}(a'e^{iP\frac{s}{2}} - b'e^{i\varphi}e^{-iP\frac{s}{2}})\,|h\rangle$$

$$\begin{aligned}&= -1/4\langle a'b'e^{-i\varphi}e^{iPs}P^2 - a'^2P^2\\ &\quad -b'^2P^2 + a'b'e^{i\varphi}e^{-iPs}P^2\rangle\\ &= 1/4\,\langle (a'^2+b'^2)P^2 - 2a'b'\cos\varphi P^2 e^{iPs}\rangle\\ &= 1/4[(a'^2+b'^2)\,\langle P^2\rangle\\ &\quad -2a'b'\,\langle\cos\varphi P^2\cos Ps\rangle]. \qquad \text{(A11)}\end{aligned}$$

The second term on the RHS of (A10) is obtained as

$$\begin{aligned}\langle\Phi|\partial_s\Phi\rangle &= \frac{i}{2}[\langle h|\,(a'e^{-iP\frac{s}{2}} - b'e^{-i\varphi}e^{iP\frac{s}{2}})\\ &\quad\times P(a'e^{iP\frac{s}{2}} + b'e^{i\varphi}e^{-iP\frac{s}{2}})\,|h\rangle]\\ &= \frac{i}{2}[\langle -a'b'e^{-i\varphi}e^{iPs}P + a'b'e^{i\varphi}e^{-iPs}P\rangle]\\ &= i\mathrm{Im}\,\langle e^{-i\varphi}e^{iPs}P\rangle\,a'b'. \qquad \text{(A12)}\end{aligned}$$

The normalization factor N is achieved as

$$N = \langle\Phi|\Phi\rangle = a'^2 + b'^2 + 2a'b'\mathrm{Re}(e^{-i\varphi}\,\langle e^{iPs}\rangle). \qquad \text{(A13)}$$

Then the Fisher information of the state $|\Phi\rangle$ can be derived as

$$\begin{aligned}F_{|\Phi\rangle}(s) &= \frac{(a'^2+b'^2)\,\langle P^2\rangle - 2a'b'\mathrm{Re}(e^{-i\varphi}\,\langle P^2e^{isP}\rangle)}{1+2a'b'\mathrm{Re}(e^{-i\varphi}\,\langle e^{iPs}\rangle)}\\ &\quad - 4\frac{(\mathrm{Im}\,\langle e^{-i\varphi}e^{iPs}P\rangle\,a'b')^2}{[1+2a'b'\mathrm{Re}(e^{-i\varphi}\,\langle e^{iPs}\rangle)]^2}. \qquad \text{(A14)}\end{aligned}$$

This allows us to compute the quantity $\langle\Phi|\Phi\rangle\,F_{|\Phi\rangle}(s)$ as

$$\begin{aligned}&(a'^2+b'^2)\,\langle P^2\rangle - 2a'b'\mathrm{Re}(e^{-i\varphi}\,\langle P^2e^{isP}\rangle)\\ &\quad -4\frac{Im^2[e^{-i\varphi}\,\langle Pe^{isP}\rangle](a'b')^2}{(a'^2+b'^2)+2a'b'Re(e^{-i\varphi}\,\langle e^{iPs}\rangle)}. \qquad \text{(A15)}\end{aligned}$$

With the above general result, we can then calculate $\langle h_1|h_1\rangle\,F_{\rho_1}$ by simply replacing a' and b' with $a\cos\alpha$ and $b\sin\alpha$, respectively:

$$\begin{aligned}\langle h_1|h_1\rangle\,F_{\rho_1} &= [(a\cos\alpha)^2 + (b\sin\alpha)^2]\,\langle P^2\rangle + 2ab\cos\alpha\sin\alpha\mathrm{Re}(e^{-i\varphi}\,\langle P^2e^{isP}\rangle)\\ &\quad -4\frac{\mathrm{Im}^2[e^{-i\varphi}\,\langle Pe^{isP}\rangle](ab\cos\alpha\sin\alpha)^2}{(a\cos\alpha)^2+(b\sin\alpha)^2-2ab\cos\alpha\sin\alpha\mathrm{Re}(e^{-i\varphi}\,\langle e^{iPs}\rangle)}. \qquad \text{(A16)}\end{aligned}$$

Similarly, we can calculate $\langle h_2|h_2\rangle\,F_{\rho_2}$ by replacing a' and b' with $a\sin\alpha$ and $b\cos\alpha$, respectively:

$$\begin{aligned}\langle h_2|h_2\rangle\,F_{\rho_2} &= [(a\sin\alpha)^2 + (b\cos\alpha)^2]\,\langle P^2\rangle - 2ab\cos\alpha\sin\alpha\mathrm{Re}(e^{-i\varphi}\,\langle P^2e^{isP}\rangle)\\ &\quad -4\frac{\mathrm{Im}^2[e^{-i\varphi}\,\langle Pe^{isP}\rangle](ab\cos\alpha\sin\alpha)^2}{(a\sin\alpha)^2+(b\cos\alpha)^2+2ab\cos\alpha\sin\alpha\mathrm{Re}(e^{-i\varphi}\,\langle e^{iPs}\rangle)}. \qquad \text{(A17)}\end{aligned}$$

Then the total Fisher information (A9) can be obtained by combining the two terms, i.e.,

$$\begin{aligned}F_{\mathrm{tot}}(s) &= \langle P^2\rangle - 4\mathrm{Im}^2[e^{-i\varphi}\,\langle Pe^{isP}\rangle]\\ &\quad\times(ab\cos\alpha\sin\alpha)^2\left(\frac{1}{N_1}+\frac{1}{N_2}\right), \qquad \text{(A18)}\end{aligned}$$

where N_1 and N_2 are given as

$$\begin{aligned}N_1 = \langle h_1|h_1\rangle &= (a\cos\alpha)^2 + (b\sin\alpha)^2\\ &\quad -2ab\cos\alpha\sin\alpha\mathrm{Re}(e^{-i\varphi}\,\langle e^{iPs}\rangle), \qquad \text{(A19)}\end{aligned}$$

$$\begin{aligned}N_2 = \langle h_2|h_2\rangle &= (a\sin\alpha)^2 + (b\cos\alpha)^2\\ &\quad +2ab\cos\alpha\sin\alpha\mathrm{Re}(e^{-i\varphi}\,\langle e^{iPs}\rangle). \qquad \text{(A20)}\end{aligned}$$

Here we analyze each of the expectation values,

$$\langle e^{iPs}\rangle = \langle h|\,e^{iPs}\,|h\rangle = e^{-s^2/8\sigma^2}, \qquad \text{(A21)}$$

$$\langle Pe^{iPs}\rangle = \langle h|\,Pe^{iPs}\,|h\rangle = \frac{-i}{4\sigma}e^{-\frac{s^2}{8\sigma^2}}s, \qquad \text{(A22)}$$

$$\langle P^2e^{iPs}\rangle = \langle h|\,P^2e^{iPs}\,|h\rangle = \frac{e^{-\frac{s^2}{8\sigma^2}}(-s^2+4\sigma^2)}{16\sigma^4}. \qquad \text{(A23)}$$

With the above results, the total Fisher information F_{tot} can finally be achieved as

$$F_{\mathrm{tot}}(s) = \frac{1}{4\sigma^2} - \frac{(r\sin\alpha\cos\alpha\cos\varphi)^2s^2}{16\left[(\cos^2\alpha + r^2\sin^2\alpha)\exp\left(\frac{s^2}{8\sigma^2}\right) - 2r\cos\alpha\sin\alpha\cos\varphi\right]}\frac{1}{\left[(r^2\cos^2\alpha+\sin^2\alpha)\exp\left(\frac{s^2}{8\sigma^2}\right)+2r\cos\alpha\sin\alpha\cos\varphi\right]}, \qquad \text{(A24)}$$

where $r = b/a$ is the unbalancedness ratio.

3. Fisher information of the unentangled field

In this section we present the derivation of the expression for FI in (7) in the main text. We consider two unentangled point sources as the superposition of $|h_\pm\rangle$ with corresponding amplitudes a and b (where $a^2 + b^2 = 1$) and a relative phase φ,

$$|\Psi'\rangle = (a\,|h_+\rangle + be^{i\varphi}\,|h_-\rangle)|\phi\rangle, \qquad \text{(A25)}$$

where $|\phi\rangle$ is a generic state of the remaining degrees of freedom. The Fisher information for the state $\rho' = |\Psi'\rangle\,\langle\Psi'|$ is defined as

$$F_{\rho'}(s) = \frac{4}{N'}\langle\partial_s\Psi'|\partial_s\Psi'\rangle - \frac{4}{N'^2}|\langle\Psi'|\partial_s\Psi'\rangle|^2, \tag{A26}$$

with the normalization factor given as

$$N' = \langle\Psi'|\Psi'\rangle = 1 + 2ab\text{Re}(e^{-i\varphi}\langle e^{iPs}\rangle). \tag{A27}$$

We can then calculate the Fisher information directly with the general result (A15) by taking $a = a'$ and $b = b'$,

$$\begin{aligned} F_{\rho'}(s) &= \frac{(a^2+b^2)\langle P^2\rangle - 2ab\text{Re}(e^{-i\varphi}\langle\Psi|P^2e^{isP}|\Psi\rangle)}{1+2ab\text{Re}(e^{-i\varphi}\langle e^{iPs}\rangle)} \\ &\quad - 4\frac{(\text{Im}\langle e^{-i\varphi}e^{iPs}P\rangle ab)^2}{[1+2ab\text{Re}(e^{-i\varphi}\langle e^{iPs}\rangle)]^2} \\ &= \frac{\frac{1}{4\sigma^2} - \cos\varphi ab e^{-\frac{s^2}{8\sigma^2}}\frac{(-s^2+4\sigma^2)}{8\sigma^4}}{1+2ab\cos\varphi e^{-s^2/8\sigma^2}} \\ &\quad - \frac{1}{4}\frac{(ab\cos\varphi e^{-\frac{s^2}{8\sigma^2}}s)^2}{(1+2ab\cos\varphi e^{-s^2/8\sigma^2})^2}. \end{aligned} \tag{A28}$$

4. Nonvanishing of the FI for unbalanced sources at $s = 0$

In this section, we show that Fisher information (5) or (A24) will never vanish at $s = 0$ for the entangled unbalanced sources. This is proved by demonstrating that the only case where $F_{\text{tot}}(s) \to 0$ (i.e., Rayleigh's curse appears) is when the two sources are balanced ($r = 1$) and at the same time the entangled partner is analyzed in the angle $\alpha = \frac{\pi}{4}$ or $\frac{3\pi}{4}$. To simplify the calculation, let's first define

$$A = r\sin 2\alpha\cos\varphi, \tag{A29}$$

$$B = \cos^2\alpha + r^2\sin^2\alpha, \tag{A30}$$

$$C = r^2\cos^2\alpha + \sin^2\alpha. \tag{A31}$$

Without loss of any generality, we then rewrite the expression for FI (A24) as

$$F_{\text{tot}}(s) = \frac{1}{4} - \frac{A^2s^2}{16(Be^{s^2/8} - A)(Ce^{s^2/8} + A)}, \tag{A32}$$

where we have taken $\sigma = 1$ for convenience. We remark that φ will be taken to be zero, which can always be realized by absorbing the additional phase in the rotated basis $|\phi_1^\alpha\rangle, |\phi_2^\alpha\rangle$ of the entangled partner.

We notice that in the limit $s \to 0$, the second term always vanishes for $(Be^{s^2/8} - A)(Ce^{s^2/8} + A) \neq 0$. This leaves the Fisher information in its maximal value ($F_{\text{tot}} = \frac{1}{4}$). Therefore, $F_{\text{tot}} = 0$ can happen only when the denominator $(Be^{s^2/8} - A)(Ce^{s^2/8} + A) = 0$ and at the same time

$$\lim_{s\to 0}\frac{A^2s^2}{16(Be^{s^2/8} - A)(Ce^{s^2/8} + A)} = \frac{1}{4}. \tag{A33}$$

There are three cases for the denominator to be zero: (i) $(Be^{s^2/8} - A) = 0$, (ii) $(Ce^{s^2/8} + A) = 0$, and (iii) both terms equal zero. According to the L'Hôpital's rule [44], for two differentiable functions $f(x)$ and $g(x)$, if $\lim_{x\to x_0} f(x) = \lim_{x\to x_0} g(x) = 0$, then $\lim_{x\to x_0}\frac{f(x)}{g(x)} = \lim_{x\to x_0}\frac{f'(x)}{g'(x)}$. Then the above limit (A33) can be converted to

$$\lim_{s\to 0}\frac{2A^2s}{16\left[B\frac{s}{4}e^{s^2/8}(Ce^{s^2/8} + A) + (Be^{s^2/8} - A)C\frac{s}{4}e^{s^2/8}\right]} = \frac{1}{4}, \tag{A34}$$

or, simply,

$$\frac{A^2}{\frac{1}{2}[B(C+A) + (B-A)C]} = 1. \tag{A35}$$

For case (i) at the limit $s \to 0$, $(Be^{s^2/8} - A) = 0$ simply means $A = B$. Then Eq. (A35) can be simplified to $A = C$. With these two conditions, we immediately achieve

$$r\sin 2\alpha\cos\varphi = r^2\cos^2\alpha + \sin^2\alpha = \cos^2\alpha + r^2\sin^2\alpha, \tag{A36}$$

where the last two terms will lead to the relation

$$\cos 2\alpha(r^2 - 1) = 0. \tag{A37}$$

From (A37), we see that $F_{\text{tot}} = 0$ can be true only when $r = 1$ or $\alpha = \frac{(4k+1)\pi}{4}$, with $k = 0, 1, 2, \ldots$ being an integer. Plugging these results back into the first two terms in (A36), we can obviously reach the conclusion that both $r = 1$ and $\alpha = \frac{k\pi}{4}$ are required for (A36) to hold.

For case (ii), we have $C + A = 0$ in the limit $s \to 0$. Then Eq. (A35) simply becomes

$$A = -B. \tag{A38}$$

With an analysis similar to that for case (i), we are led to the result that $F_{\text{tot}} = 0$ can be true only when $r = 1$ and $\alpha = \frac{(4k+1)\pi}{4}$, with $k = 0, 1, 2, \ldots$ being an integer.

For case (iii), we have both $C + A = 0$ and $B - A = 0$, which means $B = -C$. This will lead to the relation

$$\cos^2\alpha + r^2\sin^2\alpha = -r^2\cos^2\alpha - \sin^2\alpha, \tag{A39}$$

which indicates the nonphysical condition $r^2 = b^2/a^2 = -1$. Therefore, case (iii) is not a physical solution.

Combining the three cases, we can conclude that the only cases in which vanishing Fisher information ($F_{\text{tot}} = 0$) exists are in the balanced situation ($r = 1$) and when $\alpha = \frac{k'\pi}{4}$, with $k' = 1, 3, 5, \ldots$ being an odd integer. This proves the fact that the Fisher information (A24) will never vanish at $s = 0$ for any unbalanced entangled sources. In addition, for any $s > 0$, our numerical result also shows that there is no cases of $F_{\text{tot}}(s) = 0$ with the assistance of the entangled partner. This can be helpful in providing practical guidance for specific resolution problems.

5. The least resolvable distance

From Figs. 2 and 3 in the main text, we notice that the FI first experiences a decrease and then experiences an increase as the separation of the two sources increases from zero to infinity. This illustrates the existence of minimum Fisher information for a two-source separation that is the least resolvable, which we denote as s_{least}. This section provides the procedure to obtain this critical separation s_{least}.

To obtain the minimum Fisher information, we need to analyze the vanishing of the derivative of FI in (5) or (A24), i.e., $F'(s) = 0$. For the convenience of calculation we make the following simplification definitions:

$$t = \frac{1}{8\sigma^2}, \tag{A40}$$

$$X = a^2\cos^2\alpha + b^2\sin^2\alpha, \tag{A41}$$

$$1 - X = b^2\cos^2\alpha + a^2\sin^2\alpha, \tag{A42}$$

$$Y = ab\sin 2\alpha\cos\varphi. \tag{A43}$$

Then the Fisher information (A24) becomes

$$F_{\rm tot}(s) = \frac{1}{4\sigma^2} - \frac{Y^2s^2}{16\sigma^2[X\exp(ts^2) - Y][(1-X)\exp(ts^2) + Y]}$$
$$= \frac{1}{4\sigma^2} - \frac{Y^2s^2}{16\sigma^2[(X-X^2)\exp(2ts^2) + Y(2X-1)\exp(ts^2) - Y^2]}. \tag{A44}$$

This allows the computation of the derivative as

$$\frac{\partial F_{\rm tot}(s)}{\partial s} = -\frac{2Y^2s[(X-X^2)\exp(2ts^2)(1-2ts^2) + (2X-1)(1-ts^2)Y\exp(ts^2) - Y^2]}{16\sigma^2[(X-X^2)\exp(2ts^2) + Y(2X-1)\exp(ts^2) - Y^2]^2}, \tag{A45}$$

with trivial solutions of the equation $\partial F_{\rm tot}(s)/\partial s = 0$ from the above expression, i.e., $s = 0$ and $s = \infty$. The nontrivial solution of the equation requires solving the following modified equation:

$$\Lambda(s)\exp(2ts^2) + \Pi(s)\exp(ts^2) + \Omega = 0, \tag{A46}$$

where

$$\Lambda(s) = (X - X^2)(1 - 2ts^2), \tag{A47}$$

$$\Pi(s) = (2X - 1)(1 - ts^2)ab\sin 2\alpha\cos\varphi, \tag{A48}$$

$$\Omega = -(ab\sin 2\alpha\cos\varphi)^2. \tag{A49}$$

In general, this equation can be solved numerically for arbitrary parameters. As an illustration, we provide an analytical solution for the balanced two-source case, i.e., $a = b = \frac{1}{\sqrt{2}}$ or $r = 1$. In this case, we have

$$\Lambda(s, r=1) = \tfrac{1}{4}(1 - 2ts^2), \tag{A50}$$

$$\Pi(s, r=1) = 0, \tag{A51}$$

$$\Omega(r=1) = -(\sin 2\alpha\cos\varphi)^2. \tag{A52}$$

Then Eq. (A46) becomes

$$(1 - 2ts^2)\exp(2ts^2) - (\sin(2\alpha)\cos(\varphi))^2 = 0, \tag{A53}$$

which can be rewritten as

$$Z\exp(Z) = \frac{-(\sin 2\alpha\cos\varphi)^2}{e}, \tag{A54}$$

with $Z = 2ts^2 - 1$. This is a special equation with the standard solution known as the Lambert $\mathcal{W}$ function [28], i.e., $Z = \mathcal{W}(\frac{-(\sin 2\alpha\cos\varphi)^2}{e})$. Then the least resolvable distance can be achieved as

$$s_{\rm least} = \sigma\sqrt{4 + 4\mathcal{W}\left[-\frac{\sin^2 2\alpha\cos^2\varphi}{e}\right]}. \tag{A55}$$

In general, there are infinite number of branches (mostly complex functions) of the Lambert $\mathcal{W}$ function that can be denoted as $\mathcal{W}_k$, with k being an integer. In our case, the solution is purely real, and it corresponds to the case when $k = 0$, related to the principal branch of the $\mathcal{W}$ function. The behavior of this function is illustrated in Fig. 4. It is a monotonic increasing function with a minimum at $\mathcal{W}[\frac{-1}{e}] = -1$.

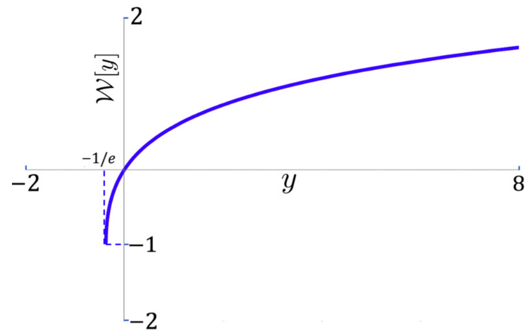

FIG. 4. Principal branch of the $\mathcal{W}$ function.

[1] E. Abbe, Beiträge zur Theorie des Mikroskops und der mikroskopischen Wahrnehmung, Archiv. f. Mikrosk. Anatomie. **9**, 413 (1873).
[2] J. W. Rayleigh, On the theory of optical images, with special reference to the microscope, London, Edinburgh, Dublin Philos. Mag. J. Sci. **42**, 167 (1896).
[3] M. Born and E. Wolf, *Principles of Optics*, 7th ed. (Cambridge University Press, Cambridge, 1999).
[4] L. Rayleigh, XXXI. Investigations in optics, with special reference to the spectroscope, London, Edinburgh, Dublin Philos. Magaz. J. Sci. **8**, 261 (1879).
[5] J. W. Goodman, *Introduction to Fourier Optics*, 1st ed. (McGraw-Hill, New York, 1968).
[6] M. I. Kolobov and C. Fabre, Quantum Limits on Optical Resolution, Phys. Rev. Lett. **85**, 3789 (2000).
[7] E. Bettens, D. Van Dyck, A. Den Dekker, J. Sijbers, and A. Van

den Bos, Model-based two-object resolution from observations having counting statistics, Ultramicroscopy **77**, 37 (1999).

[8] S. Van Aert, A. den Dekker, D. V. Dyck, and A. van den Bos, High-resolution electron microscopy and electron tomography: Resolution versus precision, J. Struct. Biol. **138**, 21 (2002).

[9] S. Ram, E. S. Ward, and R. J. Ober, Beyond Rayleigh's criterion: a resolution measure with application to single-molecule microscopy, Proc. Natl. Acad. Sci. USA **103**, 4457 (2006).

[10] J. Chao, E. S. Ward, and R. J. Ober, Fisher information theory for parameter estimation in single molecule microscopy: Tutorial, J. Opt. Soc. Am. A **33**, B36 (2016).

[11] C. Fabre, J. B. Fouet, and A. Maître, Quantum limits in the measurement of very small displacements in optical images, Opt. Lett. **25**, 76 (2000).

[12] M. Tsang, Quantum limits to optical point-source localization, Optica **2**, 646 (2015).

[13] R. Nair and M. Tsang, Far-Field Superresolution of Thermal Electromagnetic Sources at the Quantum Limit, Phys. Rev. Lett. **117**, 190801 (2016).

[14] M. Tsang, R. Nair, and X.-M. Lu, Quantum Theory of Superresolution for Two Incoherent Optical Point Sources, Phys. Rev. X **6**, 031033 (2016).

[15] M. Paúr, B. Stoklasa, Z. Hradil, L. L. Sánchez-Soto, and J. Řehácek, Achieving the ultimate optical resolution, Optica **3**, 1144 (2016).

[16] J. Řehaček, Z. Hradil, B. Stoklasa, M. Paúr, J. Grover, A. Krzic, and L. L. Sánchez-Soto, Multiparameter quantum metrology of incoherent point sources: Towards realistic superresolution, Phys. Rev. A **96**, 062107 (2017).

[17] W. Larson and B. E. Saleh, Resurgence of Rayleigh's curse in the presence of partial coherence, Optica **5**, 1382 (2018).

[18] Z. Hradil, J. Řehaček, L. Sánchez-Soto, and B.-G. Englert, Quantum Fisher information with coherence, Optica **6**, 1437 (2019).

[19] K. Liang, S. A. Wadood, and A. N. Vamivakas, Coherence effects on estimating two-point separation, Optica **8**, 243 (2021).

[20] S. A. Wadood, K. Liang, Y. Zhou, J. Yang, M. A. Alonso, X.-F. Qian, T. Malhotra, S. M. H. Rafsanjani, A. N. Jordan, R. W. Boyd, and A. N. Vamivakas, Experimental demonstration of superresolution of partially coherent light sources using parity sorting, Opt. Express **29**, 22034 (2021).

[21] M. Tsang, Resolving starlight: A quantum perspective, Contemp. Phys. **60**, 279 (2019).

[22] M. Tsang and R. Nair, Resurgence of Rayleigh's curse in the presence of partial coherence: Comment, Optica **6**, 400 (2019).

[23] C. W. Helstrom, *Quantum Detection and Estimation Theory* (Academic Press, New York, 1976).

[24] A. S. Holevo, *Statistical Structure of Quantum Theory* (Springer, Berlin, 2001).

[25] W. Larson and B. E. Saleh, Resurgence of Rayleigh's curse in the presence of partial coherence: Reply, Optica **6**, 402 (2019).

[26] S. De, J. Gil-Lopez, B. Brecht, C. Silberhorn, L. L. Sánchez-Soto, Z. Hradil, and J. Rehacek, Effects of coherence on temporal resolution, Phys. Rev. Res. **3**, 033082 (2021).

[27] A. Streltsov, G. Adesso, and M. B. Plenio, Colloquium: Quantum coherence as a resource, Rev. Mod. Phys. **89**, 041003 (2017).

[28] R. M. Corless, G. H. Gonnet, D. E. G. Hare, D. J. Jeffrey, and D. E. Knuth, On the Lambert W function, Adv. Comput. Math. **5**, 329 (1996).

[29] R. J. C. Spreeuw, A classical analogy of entanglement, Found. Phys. **28**, 361 (1998).

[30] A. Luis, Coherence, polarization, and entanglement for classical light fields, Opt. Commun. **282**, 3665 (2009).

[31] B. N. Simon, S. Simon, F. Gori, M. Santarsiero, R. Borghi, N. Mukunda, and R. Simon, Nonquantum Entanglement Resolves a Basic Issue in Polarization Optics, Phys. Rev. Lett. **104**, 023901 (2010).

[32] C. V. S. Borges, M. Hor-Meyll, J. A. O. Huguenin, and A. Z. Khoury, Bell-like inequality for the spin-orbit separability of a laser beam, Phys. Rev. A **82**, 033833 (2010).

[33] X.-F. Qian and J. H. Eberly, Entanglement and classical polarization states, Opt. Lett. **36**, 4110 (2011).

[34] K. H. Kagalwala, G. D. Giuseppe, A. F. Abouraddy, and B. E. A. Saleh, Bell's measure in classical optical coherence, Nat. Photonics **7**, 72 (2013).

[35] F. Töppel, A. Aiello, C. Marquardt, E. Giacobino, and G. Leuchs, Classical entanglement in polarization metrology, New J. Phys. **16**, 073019 (2014).

[36] F. De Zela, Relationship between the degree of polarization, indistinguishability, and entanglement, Phys. Rev. A **89**, 013845 (2014).

[37] B. Ndagano, B. Perez-Garcia, F. S. Roux, M. McLaren, C. Rosales-Guzman, Y. Zhang, O. Mouane, R. I. Hernandez-Aranda, T. Konrad, and A. Forbes, Characterizing quantum channels with non-separable states of classical light, Nat. Phys. **13**, 397 (2017).

[38] A. Z. Goldberg, P. de la Hoz, G. Björk, A. B. Klimov, M. Grassl, G. Leuchs, and L. L. Sánchez-Soto, Quantum concepts in optical polarization, Adv. Opt. Photonics **13**, 1 (2021).

[39] S. Pang and A. N. Jordan, Optimal adaptive control for quantum metrology with time-dependent Hamiltonians, Nat. Commun. **8**, 14695 (2017).

[40] D. R. M. Arvidsson-Shukur, N. Yunger Halpern, and H. V. Lepage, Quantum advantage in postselected metrology, Nat. Commun. **11**, 3775 (2020).

[41] J. Zmuidzinas, Cramér-Rao sensitivity limits for astronomical instruments: Implications for interferometer design, J. Opt. Soc. Am. A **20**, 218 (2003).

[42] S. M. Kay, *Fundamentals of Statistical Signal Processing: Estimation Theory* (Prentice-Hall, Hoboken, NJ, 1993).

[43] S. Pang, J. Dressel, and T. A. Brun, Entanglement-Assisted Weak Value Amplification, Phys. Rev. Lett. **113**, 030401 (2014).

[44] A. E. Taylor, L'Hospital's rule, Am. Math. Mon. **59**, 20 (1952).